Article

Not peer-reviewed version

Integration of Metabolomics and Transcriptomics to Explore Dynamic Alterations in Fruit Color and Quality in ‘Comte De Paris’ Pineapple during Ripening Processes

Kang Hua Song , Jia Meng Liu , Quan Sheng Yao , Yi Xing Li , Xiao Wan Hou , Sheng Hui Liu , Xun Xia Qiu , Yue Yang , Li Chen , Ke Qian Hong * , Li Jing Lin * , Xiu Mei Zhang *

Posted Date: 28 September 2023

doi: 10.20944/preprints202309.1976.v1

Keywords: pineapple; ripening; yellowing; fruit quality; metabolomics; transcriptomics

Article

Integration of Metabolomics and Transcriptomics to Explore Dynamic Alterations in Fruit Color and Quality in 'Comte de Paris' Pineapple during Ripening Processes

Kanghua Song [1,#], Jiameng Liu [2,#], Quansheng Yao [1], Yixing Li [3], Xiaowan Hou [1], Shenghui Liu [1], Xunxia Qiu [2], Yue Yang [1], Li Chen [1], Keqian Hong [1,*], Lijing Lin [2,*] and Xiumei Zhang [1,*]

[1] Key Laboratory for Postharvest Physiology and Technology of Tropical Horticultural Products of Hainan Province, South Subtropical Crop Research Institute, Chinese Academy of Tropical Agricultural Sciences, Zhanjiang 524091, China

[2] Hainan Key Laboratory of Storage & Processing of Fruits and Vegetables, Agricultural Products Processing Research Institute, Chinese Academy of Tropical Agricultural Sciences, Zhanjiang 524001, China

[3] Hainan Key Laboratory of Banana Genetic Improvement, Haikou Experimental Station, Chinese Academy of Tropical Agricultural Sciences, Haikou 571101, China

* Correspondence: hkq0825@126.com (K. Hong), linlijing0763@163.com(L. Lin), asiazhang1975@163.com (X. Zhang).

[#] These authors have contributed equally to this work

Abstract: To understand the molecular mechanism underlying yellowing in pineapples during ripening, coupled with alterations in fruit quality, comprehensive metabolome and transcriptome investigations were carried out. These investigations were conducted using the pulp samples collected at three distinct stages of maturity: young fruit (YF), mature fruit (MF), and fully mature fruit (FMF). This study revealed a noteworthy increase in the levels of total phenols and flavones, coupled with a concurrent decline in lignin and total acid content, as the fruit transitioned from YF to FMF. Furthermore, the analysis yielded 167 differentially accumulated metabolites (DAMs) and 2194 differentially expressed genes (DEGs). Kyoto Encyclopedia of Genes and Genomes enrichment analysis based on DAMs and DEGs revealed that the biosynthesis of plant secondary metabolites, particularly the flavonol, flavonoid, and phenypropanoid pathways, plays a pivotal role in fruit yellowing. Additionally, a comprehensive regulatory network encompassing genes that contribute to metabolisms of flavones, flavonols, lignin, and organic acids was proposed. This network sheds light on the intricate processes that underlies fruit yellowing and quality alterations. These findings enhance our understanding of the regulatory pathways governing pineapple ripening and offer valuable scientific insight into the molecular breeding of pineapples.

Keywords: pineapple; ripening; yellowing; fruit quality; metabolomics; transcriptomics

1. Introduction

Pineapple (*Ananas comosus* L. Merr.), a member of Bromeliaceae family, ranks as the third most commercially significant tropical and subtropical fruit globally, earning widespread acclaim for its nutrition value [1,2]. Biologically categorized as a non-climacteric species, pineapple does not undergo a post-ripening process and, post-harvest, progressively experiences a decline in quality acceptability. However, pineapple fruit ripening is accompanied by a gradual increase in respiration and ethylene release, resembling the behavior of climacteric fruits that undergo transformations in appearance, texture, and nutrient metabolism [3,4].

As aggregate fruit with a unique ripening profile, understanding the ripening characteristics of pineapple is important from both scientific and market perspectives. The transition in pulp color from white to yellow is believed to be a complex interplay of carotenoids and flavonoids, with flavonoids,

 doi:10.20944/preprints202309.1976.v1

notably flavonols, flavones, flavanols, anthocyanins, flavan-3-ols (catechins and proanthocyanidins) and phenolic acids, which are the predominant pigments [5]. The texture of fleshy fruit, a pivotal quality attribute, not only constitutes a vital component of the primary cell wall polysaccharide but also significantly contributes to fruit hardness and overall edibility [6]. Organic acids, which comprise diverse components, play a pivotal role in regulating fruit flavor. While some aspects of the content and alteration patterns of organic acids in pineapple fruit have been investigated in details [7], questions remain regarding which components change as the fruit matures and ripeness processes.

Furthermore, the biosynthesis of phenylpropanoid and phenylpropanoid, along with organic acids metabolism, coincidentally, three crucial pathways responsive to oxidative stress, result in subsequent alterations in color, texture, and flavor, driven by the production of reactive oxygen species (ROS) during pineapple fruit ripening [8,9]. For instance, redox mechanisms have been identified as critical in the ripening of the Smooth Cayenne variety [10]. Antioxidant compounds, such as flavonoids and polyphenols, have also been extensively investigated in various pineapple cultivars, including Smooth Cayenne, Red Spanish, MD-2 and Queen, during fruit ripening [11,12, 13,14], underscoring the association between ROS derived from plant secondary metabolites and diverse ripening responses.

Despite prior investigations into alterations in cellular lipids, including lipid degradation and peroxidation, during fruit ripening in 'Comte de Paris' cultivar, the chief pineapple variety cultivated in China, little is known about the molecular events and metabolites involved in transformations associated with fruit yellowing, softening, and quality improvement during ripening [15]. Therefore, the primary objective of this study was to examine ripening-related physicochemical parameters, including color, phenols, flavones, lignin, and quality. These findings were subsequently integrated with metabolomics and transcriptomics to elucidate the corresponding metabolites and genetic factors that govern fruit ripening. This comprehensive investigation is expected to significantly advance our understanding of the alterations in fruit color and quality during the fruit ripening process in 'Comte de Paris' pineapple, ultimately offering valuable insights for molecular breeding of the fruit.

2. Results

2.1. L, a*, and b* Values of Peel and Pulp*

As illustrated in Figure 1A, noticeable alterations in the morphology of both peel and pulp color were observed during the transition from green to yellow, and white to yellow, respectively, in fruit progressing from the YF stage to the FMF stage. Notably, the L* value of the peel exhibited a prominent increase, wheras the L* value of the pulp exhibited a significant decrease. These differences in L* value were statistically significant as the fruit transitioned from YF to FMF, in both peel and pulp.

Preprints (www.preprints.org) | NOT PEER-REVIEWED | Posted: 28 September 2023 doi:10.20944/preprints202309.1976.v1

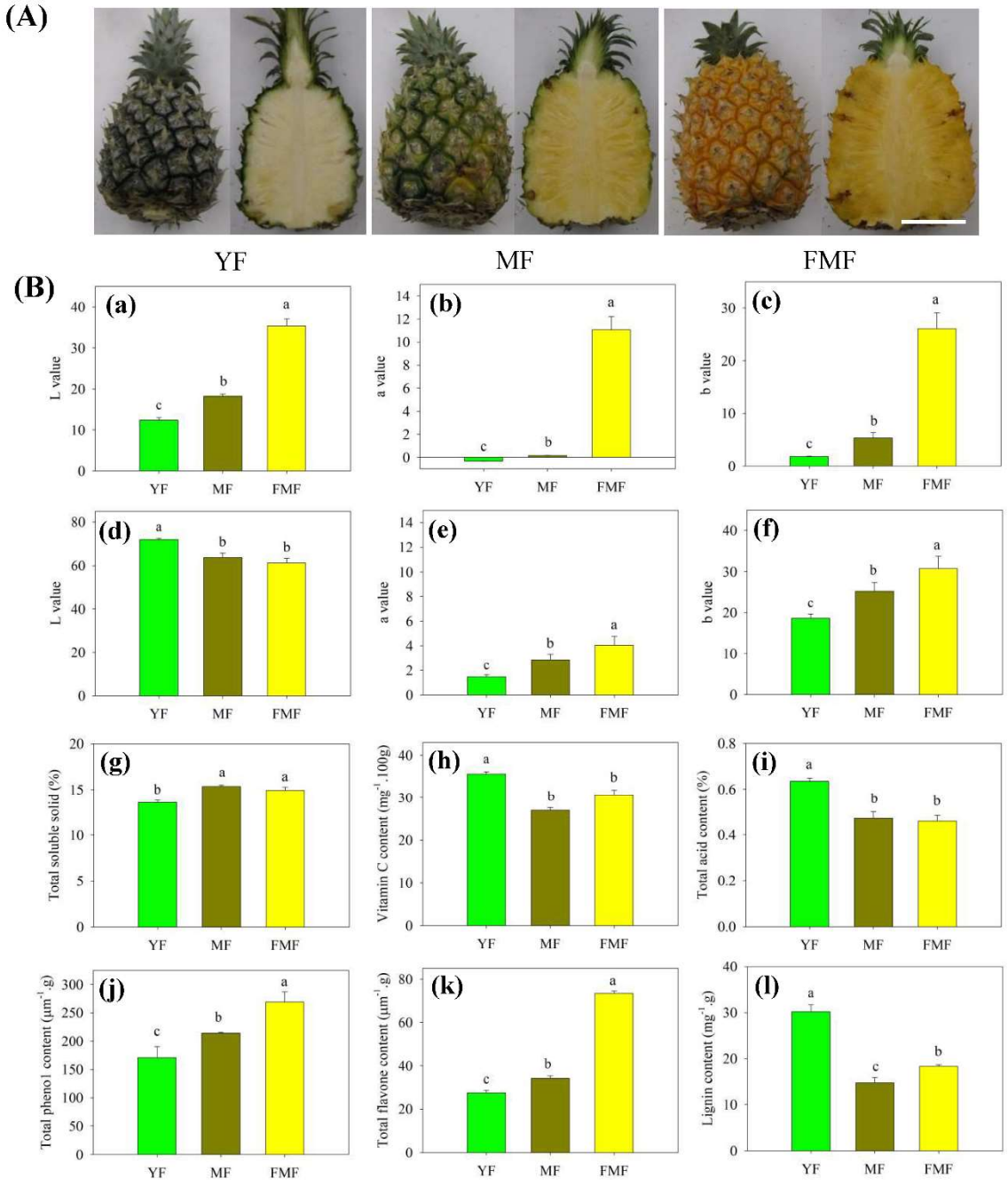

Figure 1. The changes of appearance and quality traits of pineapple fruit at three distinct stages of maturity: YF, MF, and FMF, respectively. (A) Appearance images of fruit during ripening. (B) Change in L^*, a^*, b^*, TSS, Vc content, TA, total phenolic content, total flavonoid content, and lignin content during ripening. Data are presented as the mean ± standard error derived from three independent replicates. Bars with different lower-case letters indicate significant differences based on a t-test at the $P \leq 0.05$ level. Scale bar = 8 cm.

Additionally, the values of a* and b* in both peel and pulp exhibited similar trends, consistently and significantly increasing as the ripening process advanced, as depicted in Figure 1B-a to-1B-f.

2.2. Contents of SSC, TA, and Vc in Pulp

TSS content exhibited a noteworthy increase from the YF to the MF stage, and a significant difference was observed between these two stages. However, as the fruit progressed from the MF to FMF stage, there was no substantial change in the TSS content (Figure 1B-g).

 doi:10.20944/preprints202309.1976.v1

In contrast, both TA and Vc contents displayed a marked decrease in the MF compared to YF, and subsequently, their levels remained relatively stable as the fruit matured further (Figure 1B-h and 1B-i).

2.3. Contents of Total Phenolic, Total Flavonoids and Lignin in Pulp

The contents of total phenol and flavonoids displayed a consistent trend, gradually increasing as the fruit matured. Significant differences were observed between the YF and MF stages, and between MF and FMF stages. Consequently, their contents reached higher levels in the FMF (Figure 1B-j and 1B-k).

Conversely, the accumulaton level of lignin exhibited a marked decrease in YF compared to MF. Subsequently, there was a slight increase, with significant differences detected between the MF and FMF (Figure 1B-l).

2.4. Differentially Accumulated Metabolites (DAMs) Annotated

To gain deeper insights into the metabolites associated with yellow pigment formation, softening, and acidity decrease during the ripening process, we re-evaluated the metabolomics data using YF, MF and FMF as materials [15]. By conducting a comprehensive comparison of the metabolites in the pulp of these three stages, a total of 167 DAMs were identified and categorized into various groups. These included 31 lipids, 28 organic acids, 27 phenylpropanoids, 21 flavonoids, 19 amino acids and derivatives, 10 nucleotides and derivatives, 10 alkaloids, five saccharides and alcohols, four vitamins, three tannins and nine other unclassified substances (Figure 2A).

Preprints (www.preprints.org) | NOT PEER-REVIEWED | Posted: 28 September 2023 doi:10.20944/preprints202309.1976.v1

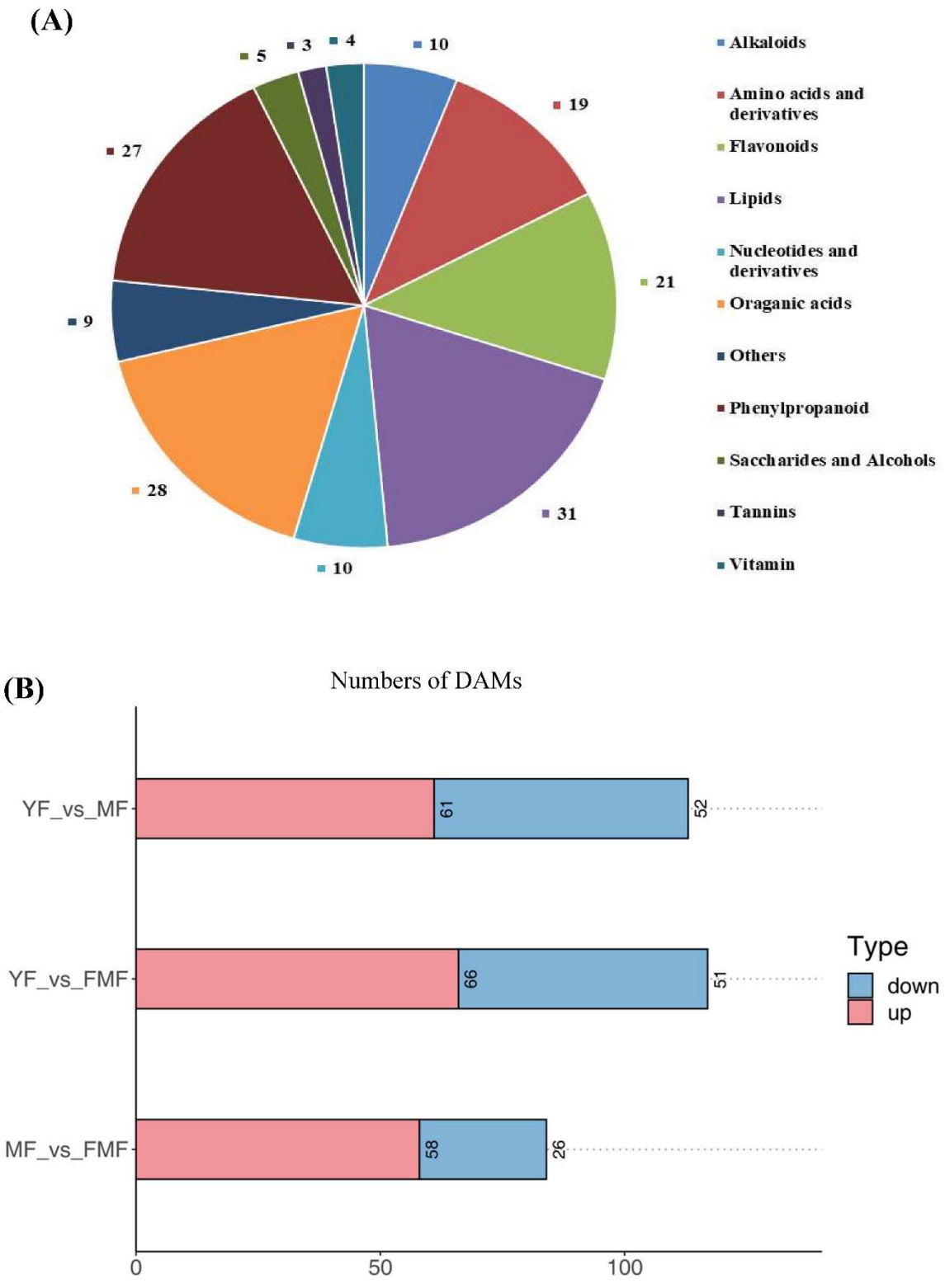

Figure 2. Analysis of 167 differentially accumulated metabolites (DAMs). (A) Pie chart of identified the types and quantities of metabolites. (B) The red and blue bars indicate the number of upregulated and downregulated DAMs between YF and MF, YF and FMF, MF and FMF, respectively.

Furthermore, we quantified the numbers of upregulated and downregulated DAMs when comparing YF to MF, YF to FMF, MF to FMF stages. Subsequently, there were 61 upregulated and 52 downregulated DAMs between YF and MF stage, 66 upregulated and 51 downregulated DAMs

Preprints (www.preprints.org) | NOT PEER-REVIEWED | Posted: 28 September 2023 doi:10.20944/preprints202309.1976.v1

between YF and FMF, 58 upregulated and 26 downregulated DAMs between MF and FMF stages (Figure 2B).

2.5. DAMs Analysis

To further elucidate the characteristics of the 167 DAMs, we conducted *K*-means clustering analysis, which result in the creation of six clusters designated C1-C6. Notably, clusters C1, C2, and C4 generally exhibited downward trends, whereas clusters C3, C5, C6 showed an upward trend during fruit ripening (Figure 3A).

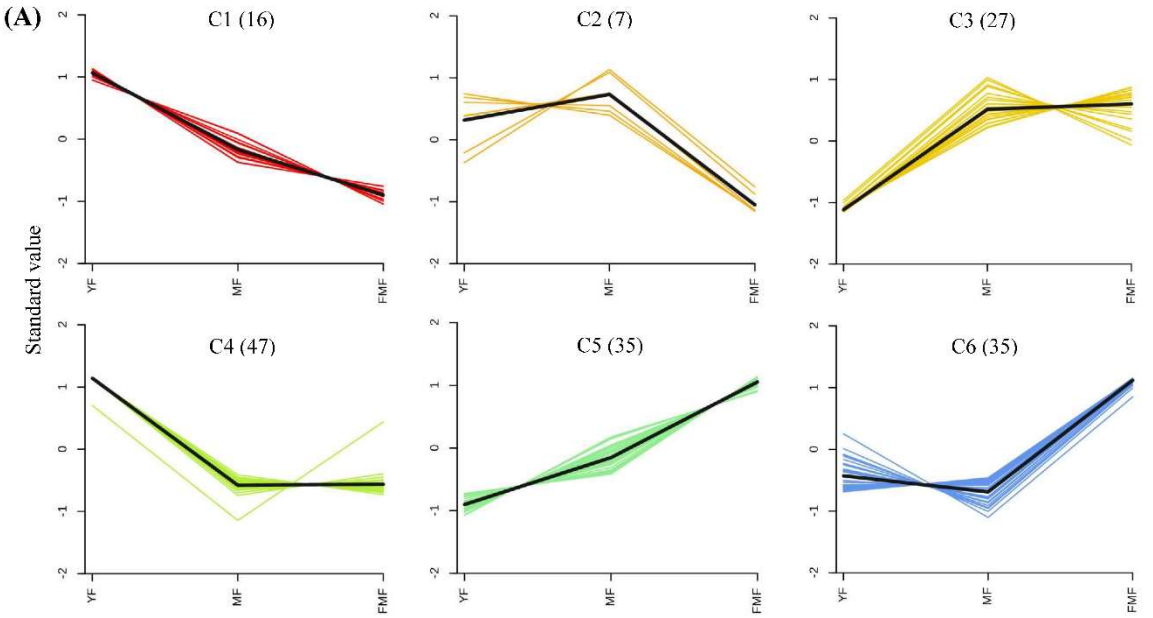

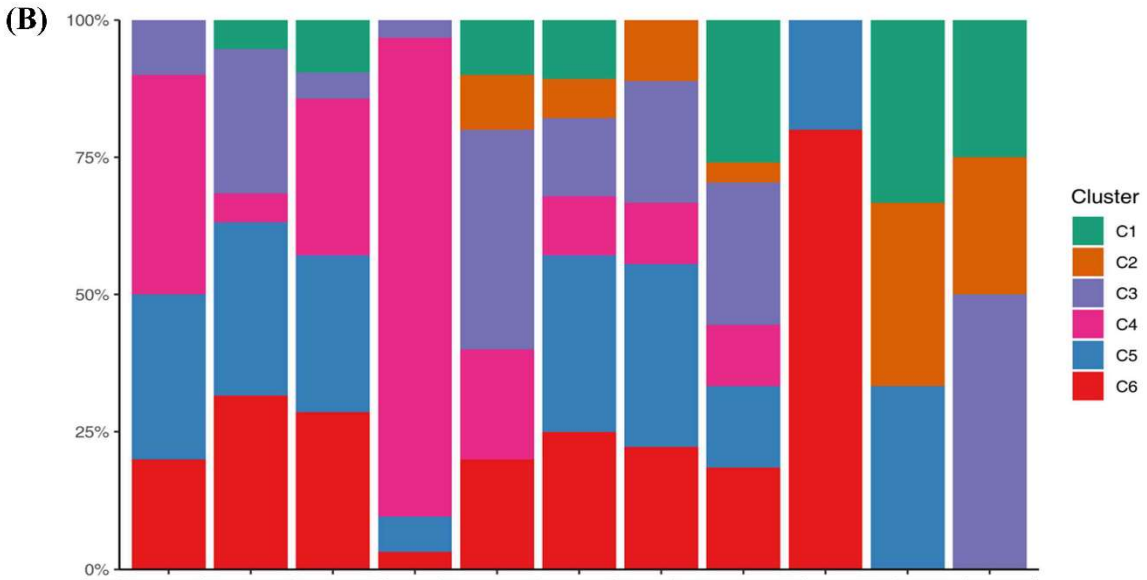

	Alkaloids	Amino acids and derivatives	Flavonoids	Lipids	Nucleotides and derivatives	Oraganic acids	Others	Phenylpropanoid	Saccharides and alcohols	Tannins	Vitamin
C1	0	1	2	0	1	3	0	7	0	1	1
C2	0	0	0	0	1	2	1	1	0	1	1
C3	1	5	1	1	4	4	2	7	0	0	2
C4	4	1	6	27	2	3	1	3	0	0	0
C5	3	6	6	2	0	9	3	4	1	1	0
C6	2	6	6	1	2	7	2	5	4	0	0

 doi:10.20944/preprints202309.1976.v1

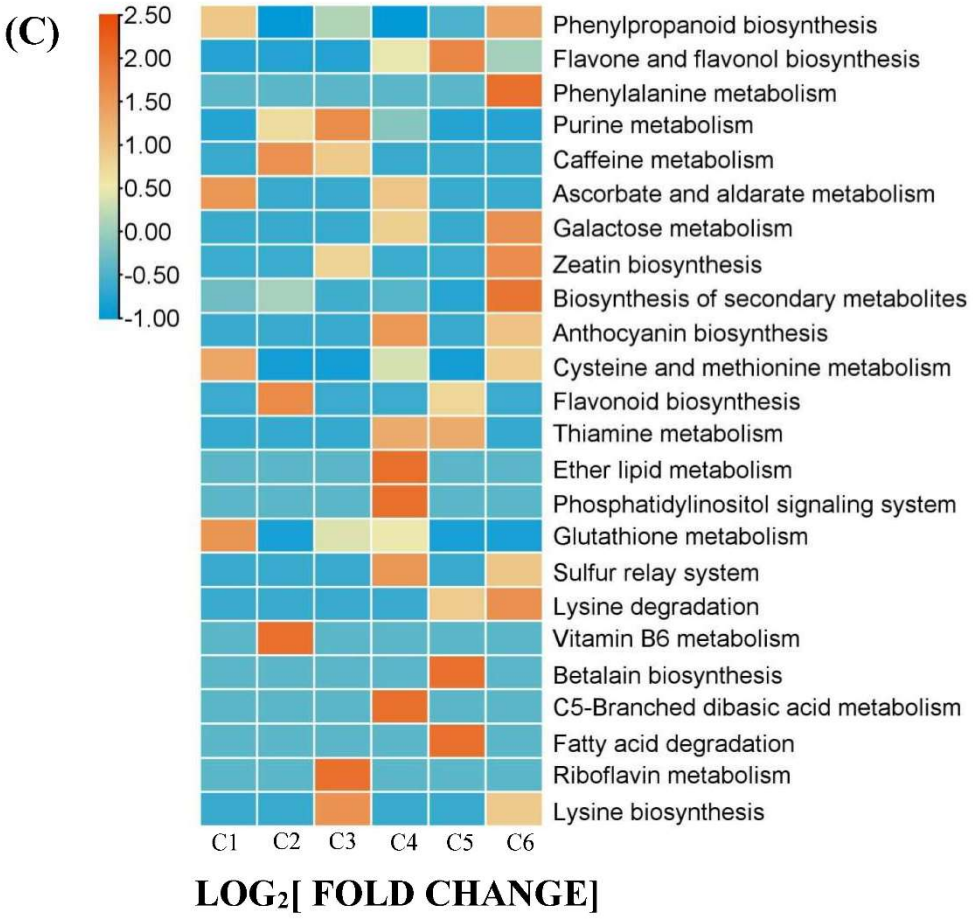

Preprints (www.preprints.org) | NOT PEER-REVIEWED | Posted: 28 September 2023 doi:10.20944/preprints202309.1976.v1

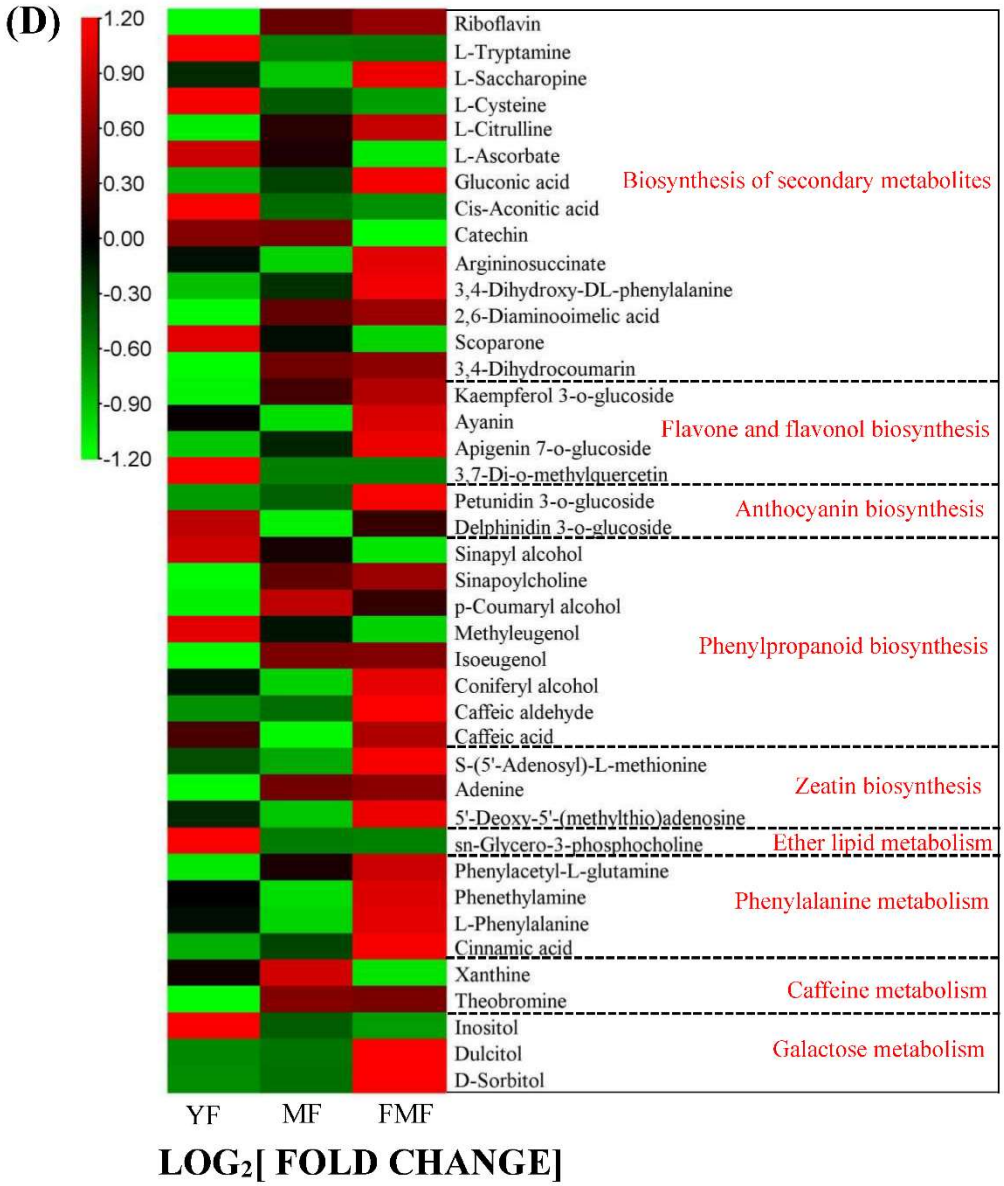

Figure 3. Overview of 167 DAMs. (A) 6 clusters of *K*-means (Designated C1-C6). (B) The distribution of different substance categories in the 6 clusters. The table below the histogram shows the number of each type of metabolites of different clusters. (C) KEGG enrichment analysis for DAMs among the 6 clusters. (D) The top of 10 pathways clustering analysis on the change trends of DAMs profiles in pineapple fruit from YF, MF, and FMF groups.

We further analyzed the distribution of metabolites from 11 categories within the C1-C6. Specifically, within the clusters showing an upward trend during fruit ripening (C3, C5, and C6), 13 flavonoids, 20 organic acids, 16 phenylpropanoids, and two vitamins displayed increasing levels as the fruit matured. Conversely, in the clusters exhibiting a downward trend (C1, C2, and C4), the levels of eight flavonoids, eight organic acids, 11 phenylpropanoids and two vitamins decreased (Figure 3B).

Furthermore, we conducted Kyoto Encyclopedia of Genes and Genomes (KEGG) enrichment analysis of 167 DAMs and performed clustering analysis to assess the changing trends of enriched pathways in the YF, MF and FMF stages. This analysis revealed that pathways such as biosynthesis of secondary metabolites, phenylpropanoid biosynthesis, flavone and flavonol biosynthesis, anthocyanin biosynthesis, and ascorbate and aldarate metabolism were significantly enriched (Figure 3C).

 doi:10.20944/preprints202309.1976.v1

Taking a closer look at the DAMs involved in the biosynthesis of secondary metabolites, we observed that organic acids such as L-ascorbate, cis-aconitic acid, rosmarinic acid, sebacate, mandelic acid, suberic acid and quinic acid O-di-glucuronic acid were degraded during the ripening of pineapple fruit. In the DAMs related to flavonoids biosynthesis, metabolites such as kaempferol 3-o-glucoside, ayanin, apigenin 7-o-glucoside, petunidin 3-o-glucoside, belonging to flavone and flavonol categories, displayed increasing trends as the fruit ripened. Conversely, within the DAMs of phenylpropanoid biosynthesis, phenols compounds, such as cinnamic acid and caffeic acid, accumulated steadily as the fruit matured. Additionally, three lignin monomers, sinapyl alcohol, *ρ*-coumaryl alcohol and coniferyl alcohol, were identified. Among these, *ρ*-coumaryl alcohol exhibited a dramatic accumulation from the MF to FMF stage, coniferyl alcohol reached its highest level in the FMF stage, and sinapyl alcohol content continuously decreased during fruit ripening (Figure 3D).

2.6. Transcriptome Profiling

2.6.1. Transcriptomics Analysis

To delve into the potential transcriptional modulatory mechanisms governing the processes of turning yellow and the alteration of fruit quality during pineapple ripening, a total of nine cDNA libraries were constructed from total RNAs for high-throughput RNA-seq analysis. After the removal of low-quality reads and adaptor sequences, the resulting total clean data ranged from 44,474,662 to 72,092,510 for each library, with a retention rate of 98.37% to 98.83%. The Q20 percentage reached 98.29% and the GC content was recorded at 52.67%. Notably, for each library, approximately 62.00% to 75.17% of clean reads were successfully mapped to the reference genome (Supplemental Table 2).

Moreover, the Principle Component Analysis (PCA) depicted in Figure 4A revealed that all biological replicates together, demonstrating high consistency among replicates. Importantly, substantial differences were observed between the YF and MF stages, YF and FMF stages, MF and FMF stages, underscoring the transcriptional variations associated with fruit ripening.

Preprints (www.preprints.org) | NOT PEER-REVIEWED | Posted: 28 September 2023 doi:10.20944/preprints202309.1976.v1

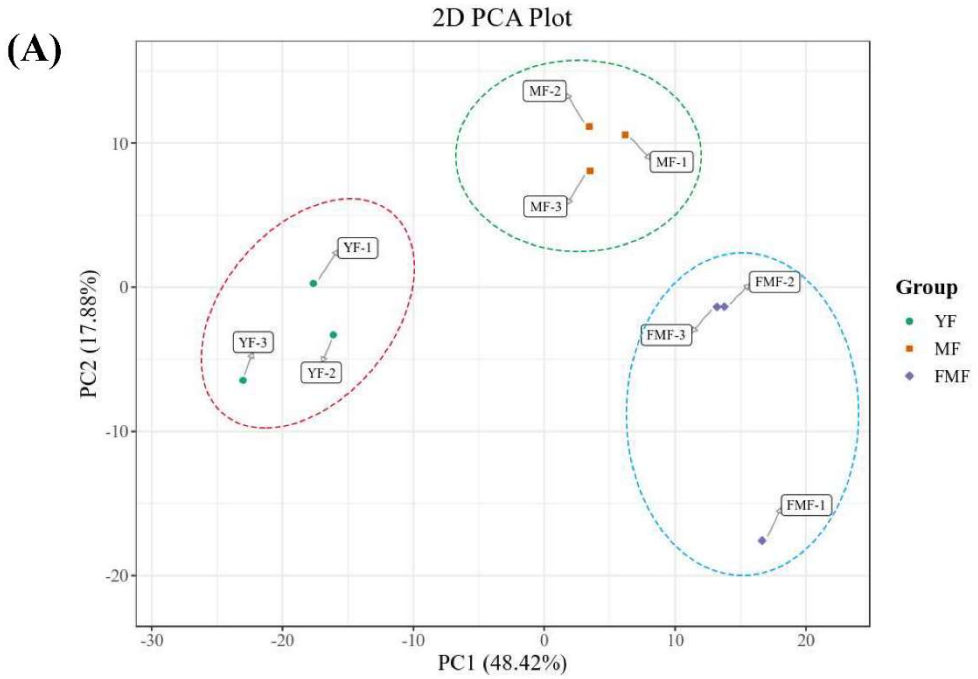

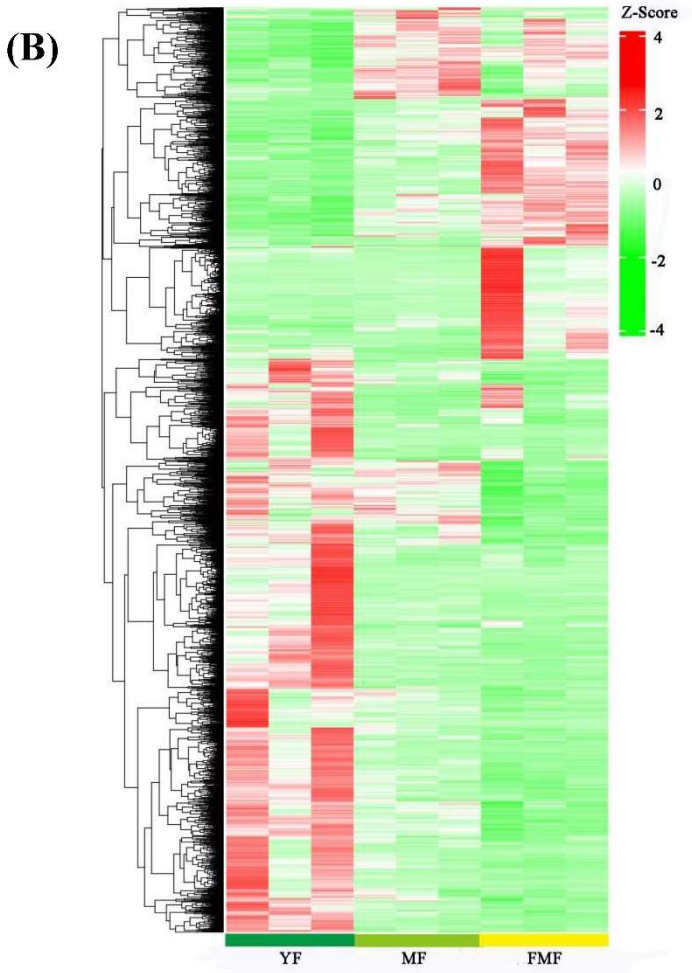

 doi:10.20944/preprints202309.1976.v1

Figure 4. Analysis of 2094 differentially expressed genes (DEGs). (A) Principal component analysis (PCA) on the RNA-seq data. (B) Hierarchical clustering analysis (HCA) of the DEGs in pineapple fruits at YF, MF, and FMF, respectively. Each gene is represented by a single row.

To further assess the differences in transcriptome profiles among the three stages (YF, MF, and FMF), we conducted Hierarchical Clustering Analysis (HCA), which resulted in the formation of three distinct clusters (Figure 4B). These findings collectively affirm the reliability of our bioinformatics analysis of our RNA-seq data obtained from different stages of pineapple fruit ripening.

2.6.2. DEGs Analysis

Applying a threshold of the log2 |Fold Change| ≥1 and FDR < 0.05, the RNA-seq data analysis identified and annotated a total of 2194 DEGs across the three samples. The results, as presented in Figure 5A and 5B, illustrate in the number of DEGs resulting from sequence comparisons between YF and MF, YF and FMF, and MF and FMF, with 989, 1796, and 707 DEGs, respectively. Notably, the largest number of DEGs was observed in the transition from YF to FMF, followed by YF to MF, and MF to FMF. This suggests that there is a greater involvement of genes in metabolic regulatory responses during the transition from MF to FMF than those of YF to MF, and MF to FMF.

 doi:10.20944/preprints202309.1976.v1

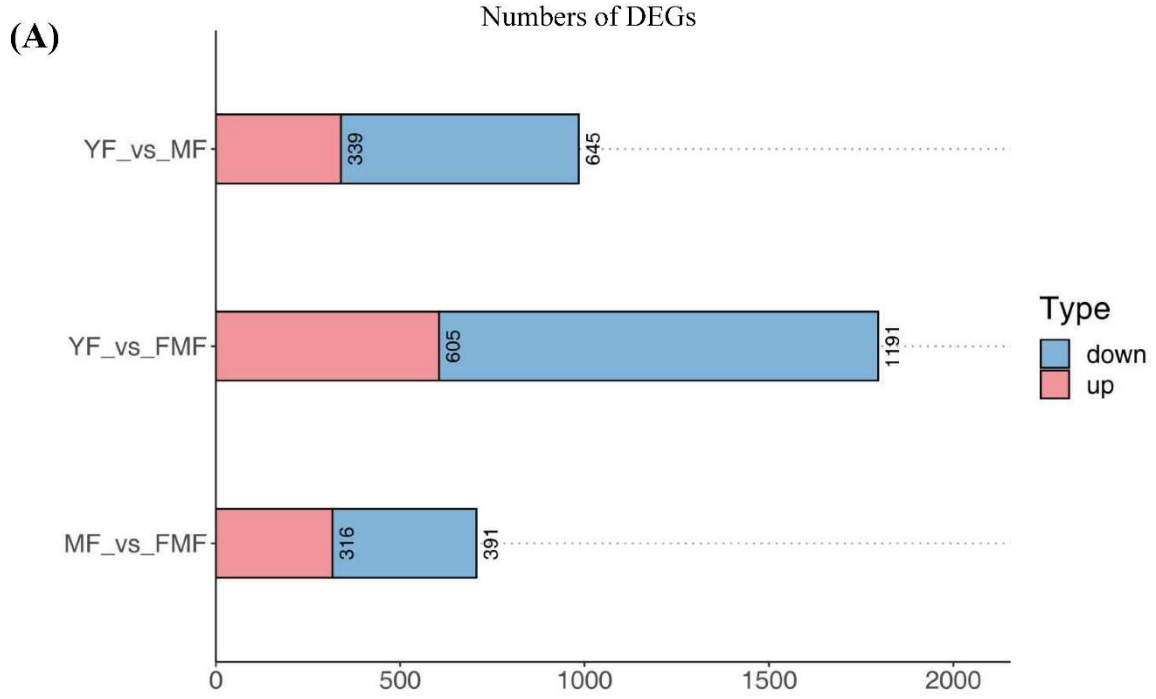

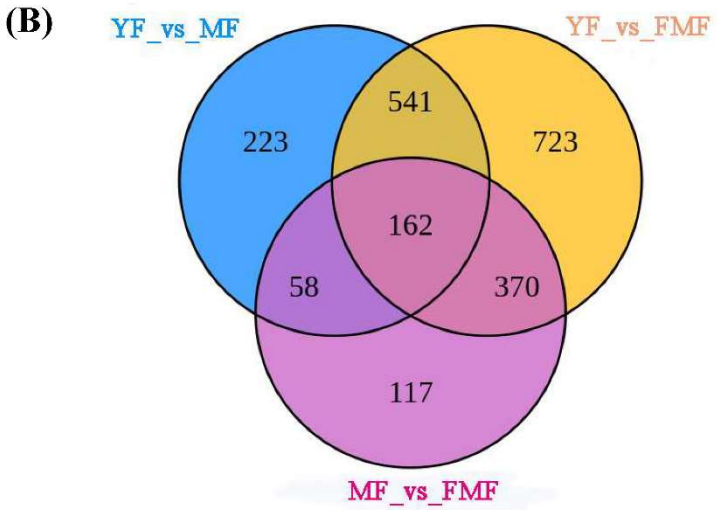

Preprints (www.preprints.org) | NOT PEER-REVIEWED | Posted: 28 September 2023 doi:10.20944/preprints202309.1976.v1

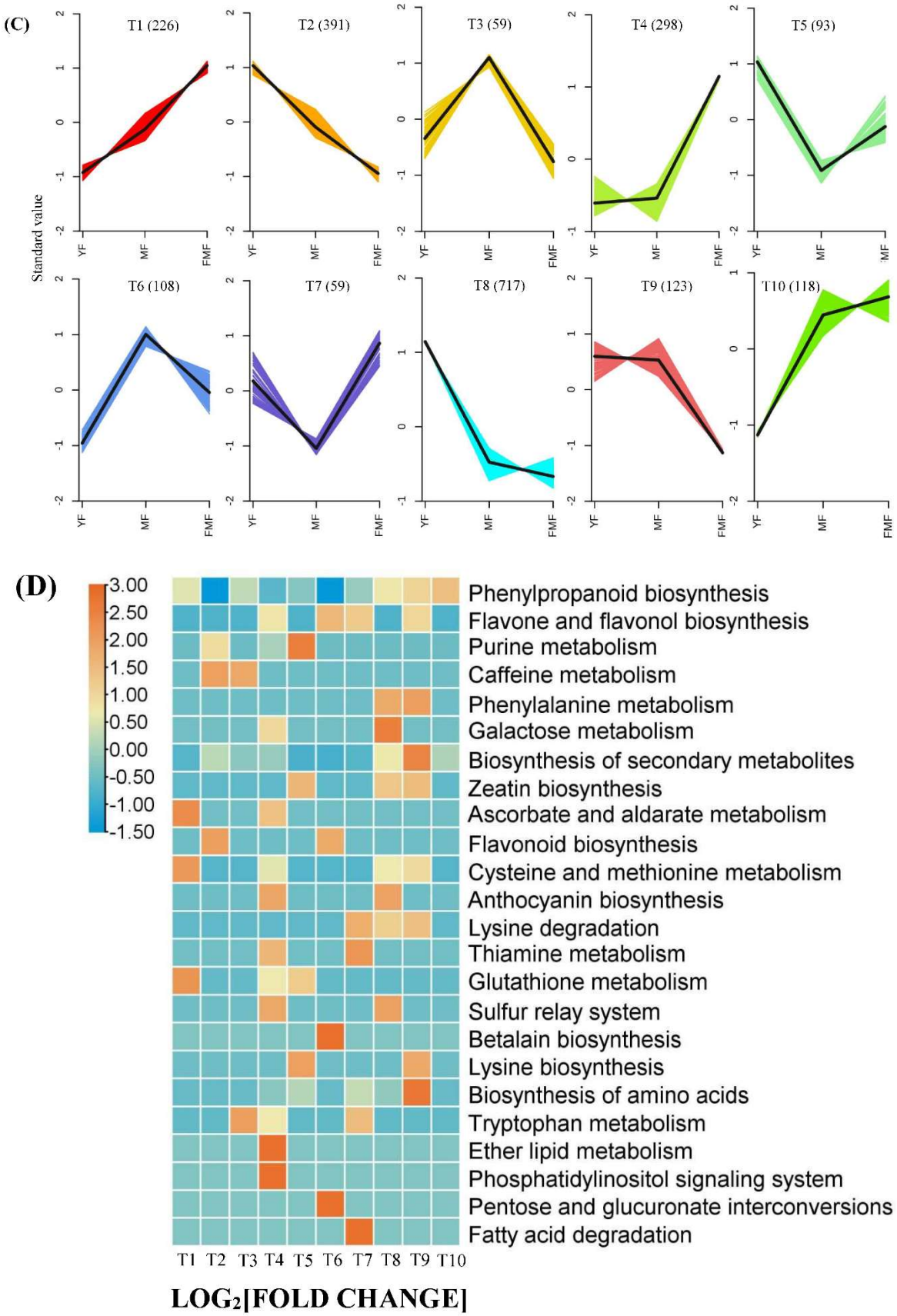

Figure 5. Overview of pineapple fruit transcriptome. (A) The red and blue bars indicate the number of upregulated and downregulated DEGs between YF and MF, YF and FMF, MF and FMF, respectively. (B) Venn diagrams illustrating the overlap of DEGs revealed by paired comparion

 doi:10.20944/preprints202309.1976.v1

between between YF and MF, YF and FMF, MF and FMF, respectively. (C) 10 clusters of K-means (Designated T1-T10). (D) KEGG enrichment analysis for DEGs among the 10 clusters.

Subsequently, we conducted *K*-means analysis of the DEGs, resulting in categorization into 10 clusters designated as T1-T10. Among these clusters, T1, T4, T6, T7, and T10 displayed upward trends in gene expression, while T2, T3, T5, T8 and T9 showed downward trends (Figure 5C).

Furthermore, we performed KEGG enrichment analysis for DEGs across the 10 clusters, revealing a significant distribution of DEGs in pathways related to biosynthesis of the secondary metabolites, phenylpropanoid biosynthesis, flavone and flavonol biosynthesis, ascorbate and aldarate metabolism (Figure 5D). These findings highlight the involvement of these pathways in the regulatory processes associated with pineapple fruit ripening.

2.7. WGCNA Analysis and Gene Network Visualization

To delve deeper into the genetic foundations governing the development of yellow pigment, softening, and acidity changes throughout the fruit ripening process, we employed WGCNA (version 1.69) to construct unsigned co-expression networks. By leveraging the identified 2194 DEGs obtained from comparative analysis across the three stages of pineapple fruit maturity, we identified six distinct gene expression modules.

Notably, four of these modules, specifically, MEblue, MEyellow, MEturquoise and MEgreen exhibited significant correlation with the changes observed in ripening-related traits, including total flavonoids content, total phenolic content, lignin levels, Vc content, and TA (Figure 6A and 6B). These correlations suggested these gene sets play a pivotal role in governing the observed alterations in pineapple fruit ripening-related traits.

Preprints (www.preprints.org) | NOT PEER-REVIEWED | Posted: 28 September 2023 doi:10.20944/preprints202309.1976.v1

(A)

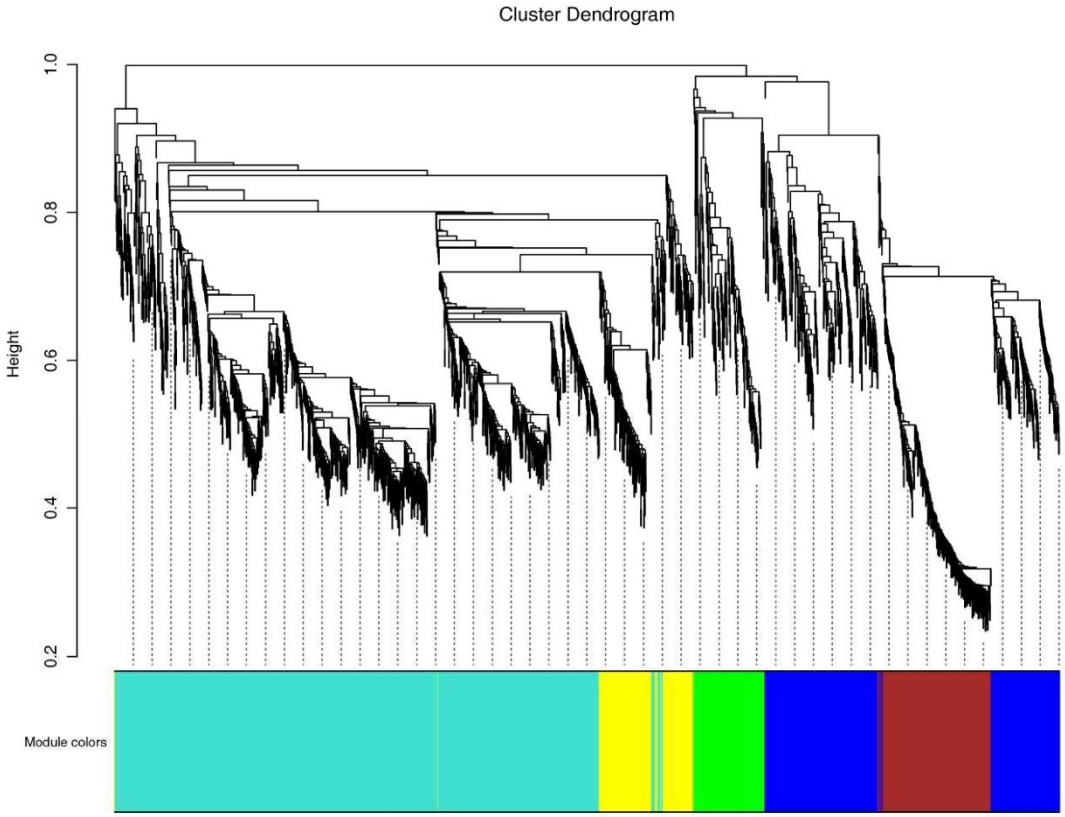

Preprints (www.preprints.org) | NOT PEER-REVIEWED | Posted: 28 September 2023 doi:10.20944/preprints202309.1976.v1

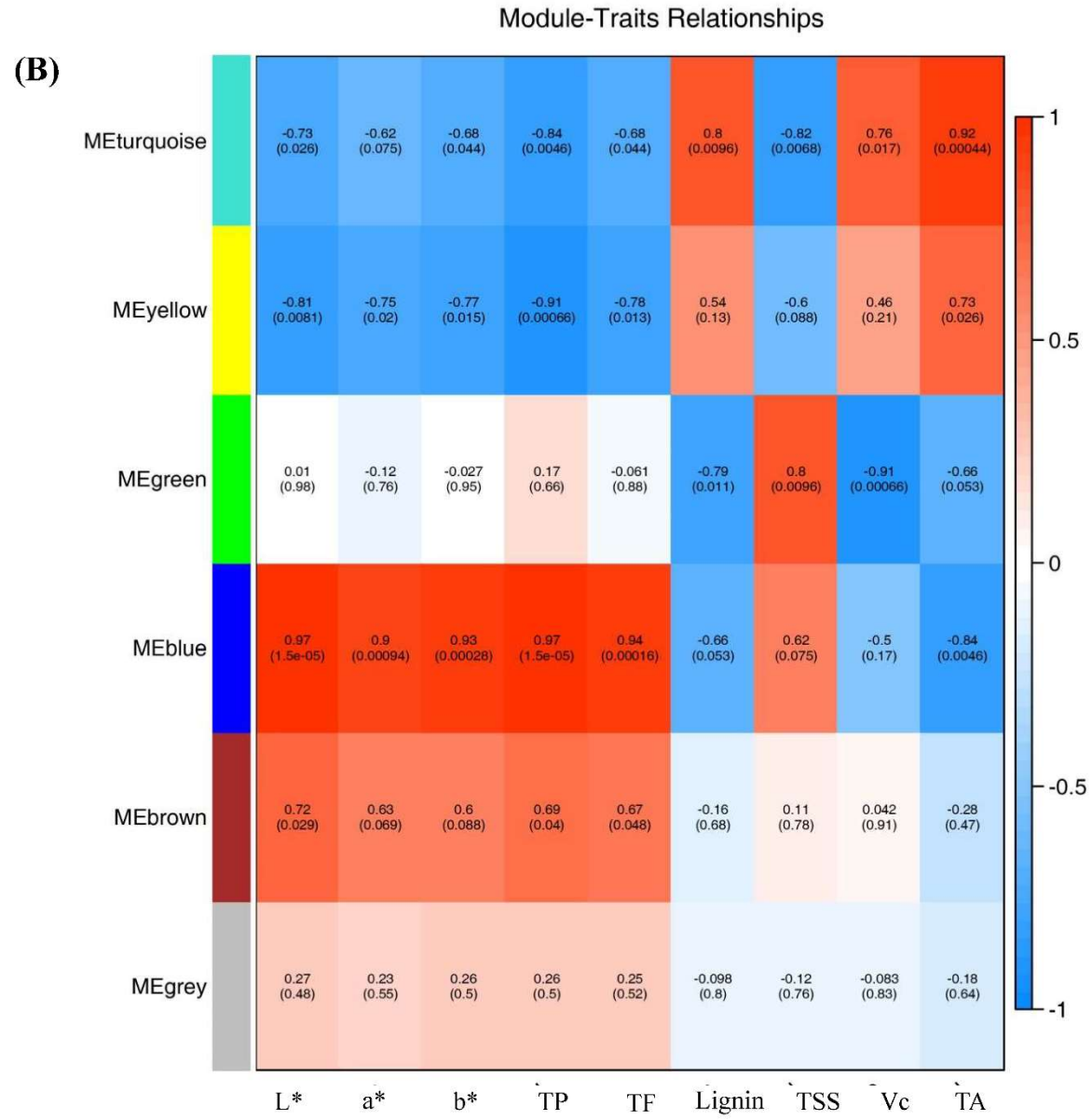

Figure 6. Correlations of 2194 DEGs with physiological indexes based on Weighted Gene Co-expression Network Analysis (WGCNA). (A). Clustering dendrogram showing 6 modules of co-expressed genes by WGCNA. (B). Module-trait relationships. Each row corresponds to a module, and each column corresponds to a quality characteristic trait. Notes: L*, L* value; a*, a* value; b*, b* value; TP, total phenols content; TF, total flavones content; TSS, total soluble solid; Vc, vitamin C content; TA, total acid.

2.8. RT-qPCR Validation of DEGs

To validate the accuracy of the RNA-seq data, we conducted RT-qPCR analysis of 14 structural genes involved in biosynthesis of flavonoids and lignin. These genes include Cinnamoyl-CoA reductase (*CCR,* Aco015695, Aco026870, Aco005397), Cinnamyl alcohol dehydrogenase (*CAD,* Aco001032), caffeic acid 3-O-Methyltranferase (*COMT,* Aco000946, Aco000839), 4-Coumaroyl CoA Ligase (*4CL,* Aco019975), Laccase (*LAC,* Aco015409), peroxidase (*POD,* Aco008456, Aco002056), flavanone 3-hydroxylase (*F3H,* Aco027900), anthocyanidin reductase (*ANR,* Aco010710), dihydroflavonol 4-reductase (*DFR,* Aco006769), glutathione S-transferase (*GST,* Aco001260).

RNA samples extracted from pineapple pulp tissues at three different ripening stages served as templates for RT-qPCR analysis. Correlation analysis revealed that a significant correlation

Preprints (www.preprints.org) | NOT PEER-REVIEWED | Posted: 28 September 2023 doi:10.20944/preprints202309.1976.v1

coefficient of 0.878 between RT-qPCR and RNA-seq was obtained by correlation analysis (Figure 7). This strong correlation suggests that the RT-qPCR results aligned well with the trends in gene expression levels detected by RNA-seq, providing additional confidence in the accuracy of the RNA-seq data.

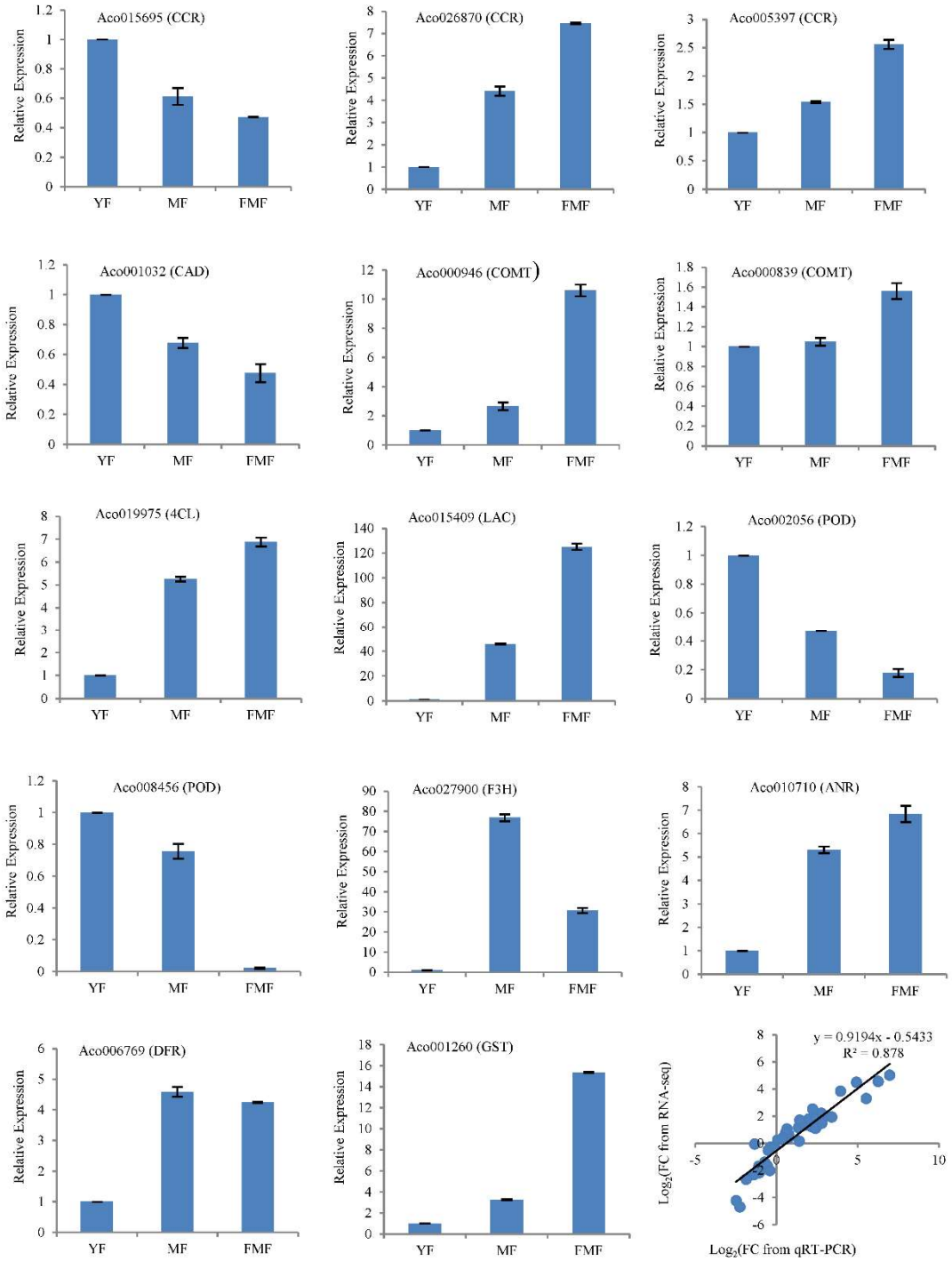

Figure 7. Verification of the RNA-seq data by RT-qPCR in 14 candidate genes involved in the biosynthesis of flavonoids and lignin. Notes: FC, fold change.

3. Discussion

In recent decades, the maturation of pineapple fruit has garnered significant attention because of its complex ripening characteristics, which vary by variety and have considerable nutritional and commercial value [10,12,13,14]. Understanding the ripening characteristics of 'Comte de Paris'

Preprints (www.preprints.org) | NOT PEER-REVIEWED | Posted: 28 September 2023 doi:10.20944/preprints202309.1976.v1

pineapple, the dominant cultivar in China, is crucial for regulating fruit quality and fostering the development of the local pineapple industry.

Fruit color, texture and taste are key indicators of fruit maturity and quality and are influenced by flavonoids, lignin, and organic acids [16]. In our study, the changing patterns of a^* and b^* values in both the peel and the pulp closely mirrored the trends in total phenol and flavonoids contents during fruit ripening. This suggests that the observed pigment variations were primarily attributable to flavonoids and total phenols biosynthesis. Conversely, the TA and lignin contents displayed similar trends, all significantly decreased from the YF stage to the MF stage (Figure 1). These findings suggest that the accumulation of flavonoids may contribute to pigment transition, which may be linked to the reduction in lignin content in cell walls, and organic acid degradation may explain the decrease in acidity during ripening. These observations are consistent with findings in other fruits, such as strawberries, papaya, and peaches [17, 18, 19].

To gain deeper insights into the metabolites associated with fruit ripening, we investigated variations in metabolites during pineapple fruit ripening. The pineapple fruit contains a variety of flavonoids that are closely linked to its color characteristics. The presence of pigments, especially flavonols and flavones, is believed to contribute to the pale-yellow pigmentation of pineapple fruit [20,21]. In our study, we observed significant increase in flavonols, such as ayanin and kaempferol 3-o-glucoside (astragalin), during fruit ripening, along with flavones, such as chrysoeriol 5-O-hexoside, chrysoeriol O-hexosyl-O-hexosyl-O-glucuronic acid, acacetin O-acetyl hexoside, apigenin 7-O-glucoside (cosmosiin), tricin O-malonylhexoside, tricin O-sinapoylhexoside, nobiletin. Additionally, other flavanones, including naringenin and hesperidin, as well as anthocyanin such as petunidin 3-O-glucoside, all exhibited continuous accumulation as fruit ripening progressed (Figure 3; Figure 8). These trends were consistent with the observed changes in fruit color and total flavonoids content. However, further research is needed to identify the specific components that contribute the most to yellow pigmentation.

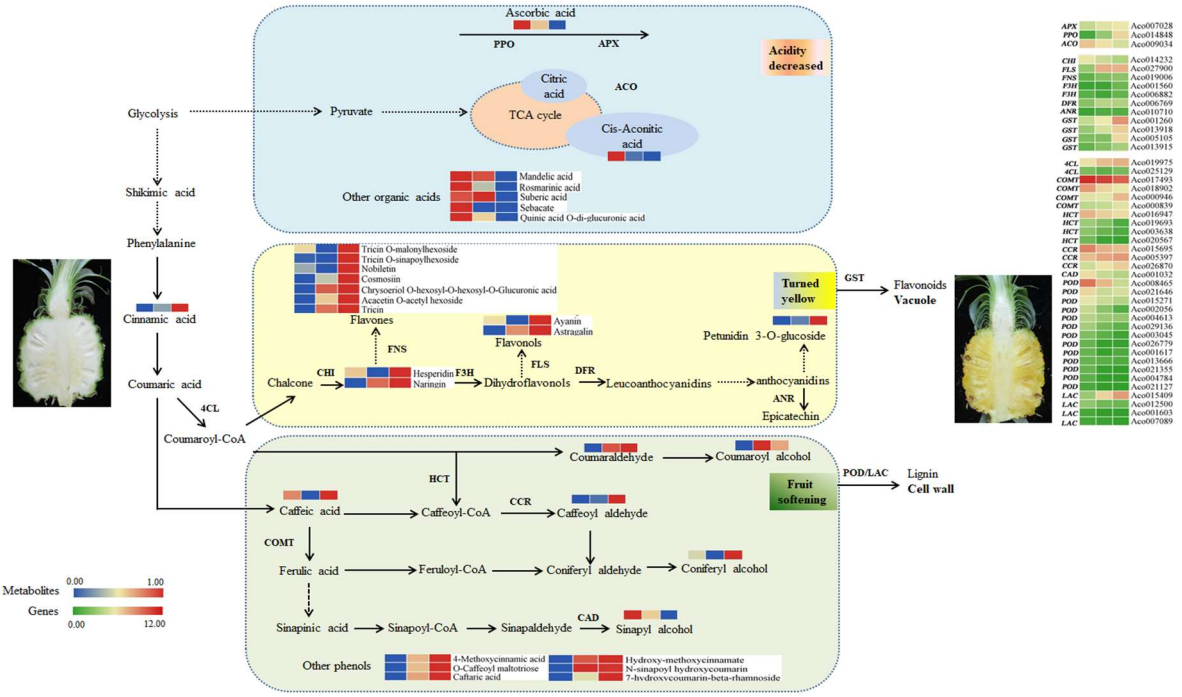

Figure 8. Dynamics of metabolites and genes related to the pineapple fruit ripening. Notes: Three blocks represent YF, MF, and FMF, respectively. SPS, sucrose phosphate synthase; APX, ascorbates peroxidase; ACO, aconitase; PPO, polyphenol oxidase; 4CL, p-coumarate: CoA ligase; CAD, cinnamyl alcohol dehydrogenase; CCR, Cinnamoyl CoA reductase; COMT, caffeic acid O-methyl transferase; HCT, hydroxycinnamoyltransferase; POD, peroxidase; LAC, laccase; CHI, chalcone isomerase; F3H, Flavanone 3-Hydroxylase; DFR, dihydroflavonol-4-reductase; ANR, anthocyanidin reductase; LDOX, leucoantho-cyanidin dioxygenase; GST, glutathione transferases.

 doi:10.20944/preprints202309.1976.v1

Fruit texture is closely correlated with lignin content in the secondary cell wall [22,23]. In this study, we identified three lignin monomers in DAMs: sinapyl alcohol, *p*-coumaryl alcohol, and coniferyl alcohol. Sinapyl alcohol exhibited a similar trend to lignin content, whereas *p*-coumaryl alcohol and coniferyl alcohol displayed opposite trend. Concurrently, phenolic compounds, such as cinnamic acid and caffeic acid, derived from phenylpropanoid biosynthesis generally increased as fruit ripening progressed, consistent with the change in total phenolic content (Figure 3). These findings suggested that these compounds play crucial roles in lignin and phenol biosynthesis.

A dramatic drop in organic acids content from YF to MF was observed in our study. Although the exact composition of the organic acids was not determined, previous research has indicated that citric acid is the predominant organic acid in mature pineapple fruit [24,25,26]. In our study, we identified cis-aconitic acid, which is an intermediate in the conversion of citric acid to isocitric acid in the tricarboxylic acid cycle, as it significantly changes with fruit ripening. Ascorbic acid, which participates in the oxidative processes during fruit ripening, also decreases during fruit ripening advanced [27]. Additionally, mandelic acid, rosmarinic acid, suberic acid, sebacate and quinic acid O-di-glucuronic acid were significantly decreased, suggesting that the reduction in TA may be attributed to the decreased content of these organic acids during pineapple fruit ripening.

Fruit ripening is a complex process involving various metabolic pathways, and reactive oxygen species (ROS) play a crucial role in ripening tropical and subtropical fruits [4]. In the present study, we aimed to clarify the role of ROS in fruit ripening by investigating the pathways related to the biosynthesis of flavonoids, lignin, and the consumption of organic acids. Candidate genes associated with ripening characteristics, such as total flavonoids, total phenolic content, lignin, Vc, and TA, were identified using WGCNA.

The biosynthesis of flavonoid has been well-documented from a molecular genetic perspective [28,29]. Chalcone isomerase (CHI) catalyzes the conversion of colorless chalcones to flavanone (naringenin). In monocots, naringenin is further metabolized into flavones by flavone synthase (FNS), where F3H and flavonol synthase (FLS) are required for the synthesis of dihydroflavonols and flavonols [30]. In some plant tissues such as fruits, DFR competitively reduces dihydroflavonols to leucoanthocyanidins, which are then converted to proanthocyanidins by ANR [24]. GST is responsible for transferring anthocyanins, flavonols and flavones into the vacuole or cell wall for storage [31,32]. In our study, nine oxidoreductase genes including *FLS* (Aco027900), *FNS* (Aco019006), *F3H* (Aco001560, Aco006882), *DFR*(Aco006769), *ANR*(Aco010710), and *GST* (Aco001260, Aco013918, Aco005105, Aco013915), were identified by WGCNA (Figure 6). These genes exhibited significantly and continuously increasing expression during fruit ripening, correlating with the accumulation of flavones and flavonols, which contribute to pigment formation.

Phenylpropanoid metabolism is closely associated with lignin biosynthesis. In this pathway, 4-Coumaroyl CoA Ligase (4CL) catalyzes the formation of activated thioesters of hydroxycinnamic acids, which enter different branch pathways of phenylpropanoid metabolisom [33]. Hydroxycinnamoyl CoA: shikimate hydroxycinnamoyl transferase (HCT) is a key metabolic entry point for the synthesis of essential lignin monomers, coniferyl and sinapyl alcohols, particularly in monocotyledonous plant [34]. COMT methylates caffeic acid to ferulic acid, whereas CCR and CAD convert CoA ester to alcohol during monolignol biosynthesis. These monolignols are exported to the cell wall and polymerized into lignin by POD or depolymerized by LAC [35, 36]. In our study, four hydroxycinnamoyl transferase (HCT) genes were downregulated during fruit ripening, consistent with the accumulation of *p*-coumaryl alcohol and the reduction of lignin monomers, coniferyl, and sinapyl alcohols. The expression of screened *COMT* (Aco017593, Aco018902), *CCR* (Aco015695), and *CAD* (Aco001032) genes generally showed a decreasing trend, in line with the accumulation of intermediate phenolic metabolites such as caffeic acid and caffeoyl aldehyde. Additionally, identified *POD* genes (Aco008465, Aco021646, Aco015271, Aco002056, Aco004613, Aco029136, Aco003045, Aco026779, Aco001617, Aco013666, Aco021355, Aco004784, Aco021127) and the *LAC* gene (Aco015409) were downregulated during fruit ripening (Figure 8), indicating their potential role in the depolymerization of lignin in the cell wall as fruit ripening progressed.

 doi:10.20944/preprints202309.1976.v1

Ascorbic acid is known to be oxidized to dehydroascorbic acid during fruit ripening, a process catalyzed by ascorbic acid oxidase (APX) [10,27,37]. In our study, genes related to *APX* (Aco007028), and polyphenol oxidase (*PPO*, Aco014848) exhibited consistently increasing expression as fruit ripening progressed, suggesting their involvement in the oxidation of ascorbic acid. Cis-aconitic acid, an organic acid is catalyzed by the aconitase (ACO), which converts citric acid to isocitric acid [38]. In our study, the expression of *ACO* (Aco009034) gradually decreased (Figure 8), suggesting its potential role in the reduced accumulation of cis-aconitic acid during pineapple fruit.

Based on these findings, we propose a schematic overview to elucidate the metabolites and corresponding genes involved in pineapple fruit ripening (Figure 8). Further research is required to fully understand the regulatory mechanisms underlying these processes.

4. Materials and methods

4.1. Plant Materials and Sampling

Pineapple (*Ananas comosus* cv. 'Comte de Paris') fruits, carefully selected for their absence of defects and mechanical damage, were procured from a commercial orchard in Xuwen county (20°34′N; 110°17′E), Zhanjiang city, Guangdong province, China, in September 2018. These fruits were swiftly transported to the laboratory within a two-hour timeframe. A total of 120 fruits were used in this experiment, meticulously chosen to represent three distinct stages of maturity: young fruit (YF), mature fruit (MF) and fully mature fruit (FMF), with 40 fruits allocated to each stage. The definition of maturity stage followed the criteria established in our previous study [15]. To ensure robustness, three replicate samples were meticulously prepared for each biological sample, with 12 fruits sampled from each replicate to assess the physiological parameters. Fruit pulp weighing 20.0 grams was collected following the methodology outlined in our previous work [39] and stored at -80 ℃ for subsequent assessments.

4.2. Evaluation of the Color Changes of Fruit

The color-related parameters, including L* (presenting lightness), a* (indicating the transition from green to red), and b* (indicating the shift from blue to yellow) were measured using a high-precision colorimeter (HP-C210, Shanghai, China). To assess L*, a* and b*, at least nine fruits at each ripening stage were halved longitudinally along the equator of the peel and pulp. At this juncture, three distinct points were selected for each parameter and readings for L*, a*, and b* were recorded. For each pineapple, three readings were captured for each color-related parameter, ensuring robust and reliable measurements.

4.3. Measurements of Contents of Soluble Solids, Titratable Acid, and Vitamin C in Pulp

The total soluble solids content (TSS) was analyzed using a handheld PAL-1(B625333) device, and the values were expressed in degree Brix.

For titratable acid (TA) determination, we followed the acid-base titration method outlined by Li et al. [40]. Briefly, 3 grams of frozen pulp power was dissolved in 30 mL distilled water and then heated to 80 ℃ for 30 min. After centrifugation at 4000 × *g* for 15 min, 10 mL of the supernatant was titrated with 0.1 mol L^{-1} NaOH, and the titration volume was recorded. The resulting data are expressed as the percentage of citric acid.

To determine the Vitamin C (Vc) content, we employed a titration method utilizing 2, 6-dichlorophenol indophenols following the procedure described by Hou et al. [41]. In short, 3 grams of frozen pulp tissue was ground in 25 mL of 2% oxalic acid solution on ice, followed by centrifugation at 4000 × *g* at 4 ℃ for 15 min. The supernatant was then titrated with 2,6-dichlorophenol indophenol, and the results were expressed as grams per kilogram (g kg^{-1}) of fresh weight (FW).

4.4. Extractions and Assays of Contents of Total Phenolic, Total Flavonoids and Lignin in Pulp

 doi:10.20944/preprints202309.1976.v1

The total phenolic content was determined using the Folin-Ciocalteu method, as outlined in Zhou et al. [42], with slight modification. In brief, 0.5 grams of frozen pulp tissue was homogenized in 80% (v/v) methanol for 2 h and subsequently centrifuged at 10, 000 × g for 15 min. The supernatant solution was collected for the analysis of total phenolic and flavonoids contents. A mixture consisting of 0.5 mL supernatant, 2 mL of Folin-Ciocalteu reagent, and 2 mL of 7.5% (w/v) Na_2CO_3 was incubated at 50 °C for 5 min. The absorbance was measured at 760 nm and the results were expressed as grams of gallic acid equivalent per kilogram (g of gallic acid equivalent kg^{-1}) of FW.

Total flavonoids content was determined using the aluminum nitrate method, as described by Zhou et al. [42]. In summary, 3 mL of supernatant, 0.5 mL 5% (w/v) $NaNO_2$ and 0.5 mL 10% (w/v) $AlNO_3$ were mixed. After 5 min, 1 mL of 1 mol L^{-1} NaOH was added. The absorbance was measured at 510 nm and the results were calculated based on a standard curve and defined as g rutin kg^{-1} FW.

To determine lignin content, a modified version of the procedure described by Morrison [43] was employed. Approximately 5 grams of pulp tissues powder was mixed with 95% pre-cooled ethanol, then centrifuged at 12,000 × g for 30 min at 4 °C, and this process four times. Sediment was collected and dried overnight at 70 °C. Subsequently, 0.1 grams of residue was dissolved in 1 mL of 25% (v/v) acetyl bromine-acetic acid, and the solution was incubated at 70 °C for 30 min. After cooling on ice, the reaction was terminated with 1 mL of 2 mol L^{-1} NaOH, followed by addition 2 mL of glacial acetic acid and 0.1 mL of 7.5 mol L^{-1} hydroxylamine hydrochloride (7.5 mL). After centrifugation at 12,000 × g and 4 °C for 10 min, the absorbance was measured at 280 nm. The lignin content was then calculated against the standard curve and expressed as g.kg-1 of FW.

4.5. RNA Extraction, Illumine Sequencing and Transcriptomics Data Analysis

Total RNA was meticulously extracted from pulp tissues representing three distinct ripening stages, following the manufacturer's instructions, using a Quick RNA isolation kit (Huayueyang, China). RNA quality was comprehensively assessed using a 2100 Bioanalyzer RNA Nanochip (Agilent, USA). To confirm RNA integrity, electrophoresis was performed on formaldehyde-containing 1.5% (w/v) agarose gels.

For library preparation, all procedures were performed in strict accordance with the manufacturer's guidelines provided with the Truseq2 RNA sample prep Kit from Illumina, Inc. San Diego, CA, USA. Raw data were acquired using the Illumina HiSeq TM2000 platform and subsequently aligned to the pineapple reference genome using HISAT2.

To identify differentially expressed genes (DEGs) among samples, transcript abundance was estimated using the fragments per kilobase of exon per million mapped reads method. Statistically significant DEGs were identified based on the criteria of False Discovery Rate (FDR) ≤ 0.05, $|\log_2 ratio| \geq 1$. *K*-means cluster analysis was carried out using the R package, and enrichment analysis of DEGs was performed using a hypergeometric distribution test. Gene expression patterns were visualized and presented using TBtools.

4.6. Weighted Gene Co-expression Network Analysis and Gene Network Visualization

A total of 2194 DEGs were employed to construct unsigned co-expression networks using the Weighted Gene Co-expression Network Analysis (WGCNA) tool, version 1.69 [44]. The followings parameters were applied: the power of 14, maximum module size of 5000, minimum module size of 30, and merge height of 0.25. For each module, the eigengene value was calculated and subsequently used to assess correlations with ripening properties including L^*, a^*, b^*, total phenolic content, total flavonoid content, lignin content, TSS, Vc content, and TA. The co-expression diagram was visually represented using Cytoscape, version 3.8.1.

4.7. Quantitative Real-Time PCR (RT-qPCR) Verification

Fourteen candidate genes involved in the biosynthesis of flavonoids and lignin were selected randomly for verification using RT-qPCR, with three biological replicates. *Acactin* (HQ148720) was used as an endogenous reference gene, and gene-specific primer sequences are shown in

Supplemental Table 1. The relative expression of these candidate genes was determined using the $2^{-\triangle\triangle CT}$ method following the approach outlined by Livak and Schmittgen [45].

4.8. Statistics

Statistics analysis was performed using one-way analysis of variance (ANOVA) with SPSS (version 16.0, Chicago, IL, USA). Data are presented as the mean ± standard error derived from three independent replicates. Statistically significant differences were assessed using the least significant difference test, with the significance set at $P < 0.05$.

5. Conclusion

The data presented in this study revealed significant changes in pineapple ripening, including the development of yellow pigment, softening of the fruit, a decrease in acidity. Metabolomic analyses have provided insights into the underlying mechanisms responsible for these changes. Specifically, the observed phenomenon can be attributed to the following:

Increased Accumulation of Flavonoids: The ripening process is associated with a notable increase in flavonoid content, including ayanin, kaempferol 3-o-glucoside, chrysoeriol 5-O-hexoside, chrysoeriol O-hexosyl-O-hexosyl-O-glucuronic acid, acacetin O-acetyl hexoside, apigenin 7-O-glucoside, tricin O-malonylhexoside, tricin O-sinapoylhexoside, nobiletin, naringenin and hesperidin.

Reduction of Lignin: Lignin content decreases during ripening, with sinapyl alcohol identified as a significant component involved in this process.

Degradation of Organic Acids: The levels of various organic acids, including cis-aconitic acid, mandelic acid, rosmarinic acid, suberic acid, sebacate and quinic acid O-di-glucuronic acid, decreased as the fruit ripened.

Furthermore, the integration of metabolomic and transcriptomic data has identified a series of putative candidate genes associated with the metabolism of flavonoids, lignin and organic acids. These candidate genes included the following:

Flavonoid Metabolism:

FLS (Aco027900), *FNS* (Aco019006), *F3H* (Aco001560, Aco006882), *DFR*(Aco006769), *ANR*(Aco010710), and *GST* (Aco001260, Aco013918, Aco005105, Aco013915).

Lignin Metabolism:

COMT (Aco017593, Aco018902), *CCR* (Aco015695), *CAD* (Aco001032), *POD* genes (Aco008465, Aco021646, Aco015271, Aco002056, Aco004613, Aco029136, Aco003045, Aco026779, Aco001617, Aco013666, Aco021355, Aco004784, Aco021127), and *LAC* (Aco015409).

Organic acid Metabolism:

APX (Aco007028), *PPO* (Aco014848), and *ACO* (Aco009034).

These identified genes are inferred to play crucial roles in regulating the changes in fruit color and quality during pineapple ripening. The insights gained from this study will contribute to better understanding of the molecular mechanisms underlying these ripening processes. This knowledge can serve as a scientific foundation for genetic breeding efforts aimed at improving pineapple fruit quality.

Acknowledgements: This research was supported by Science and Technology special fund of Hainan Province (No. ZDYF2021XDNY303), Central Public-interest Scientific Institution Basal Research Fund (No. 1630062022006), Natural Science Foundation of Hainan Province (No. 321QN0921; No. 320MS087), and Central Public-interest Scientific Institution Basal Research Fund for Chinese Academy of Tropical Agricultural Sciences (No. 1630062023005).

References

1. Sun, G.M.; Zhang, X.M.; Soler, A.; Marie-alphonsine, P.A. Nutritional composition of pineapple (*Ananas comosus* (L.) Merr.). *Nutritional Composition of Fruit Cultivars*. **2016**, 609-637. http://doi.org/10.1016/B978-0-12-408117-8.00025-8

2. Ali, M.M.; Hashim, N.; Aziz, S.A.; Lasekan, O. Pineapple (*Ananas comosus*): A comprehensive review of nutritional values, volatile compounds, health benefits, and potential food products. *Food Res. Int*. **2020**, 137, 109675. http://doi.org/10.1016/j.foodres.2020.109675
3. Shuvo, M.S.H.; Rahman, S.B.; Mortuza, M.G.; Rahman, M.A. Changes in physicochemical properties of pineapple at different ripening stages during storage. *J. Agrofor. Environ*. **2019**, 13, 1-2. http://jagroforenviron.com
4. Li, L.; Yi, P.; Sun, J.; Tang, J.; Liu, G.M.; Bi, J.F.; Teng, J.W.; Hu, M.J.; Yuan, F.; He, X.M.; Sheng, J.F.; Xin, M.; Li, Z.C.; Li, C.B.; Tang, Y.Y.; Ling, D.N. Genome-wide transcriptome analysis uncovers gene networks regulating fruit quality and volatile compounds in mango cultivar 'Tainong' during postharvest. *Food Res. Int*. **2023**, 165, 112531. http://doi.org/10.1016/j.foodres.2023.112531
5. Hassan, A.; Othman, Z.; Siriphanich, J. Pineapple (*Ananas comosus* L. Merr.). *Postharvest Biology and Technology of Tropical and Subtropical Fruits*. **2011**, 218e, 194-217. http://doi.org/10.1533/9780857092618.194
6. Hu, Y.J.; Cheng, H.; Zhang, Y.; Zhang, J.; Niu, S.Q.; Wang, X.S.; Li, W.J.; Zhang, J.; Yao, Y.C. The MdMYB16/MdMYB1-miR7125-MdCCR module regulates the homeostasis between anthocyanin and lignin biosynthesis during light induction in apple. *New Phytol*. **2021**, 231, 1105-1122. http://doi.org/10.1111/nph.17431
7. Zhang, X.X.; Wei, X.X.; Ali, M.M.; Rizwan, H.M.; Li, B.Q.; Li, H.; Jia, K.J.; Yang, X.L.; Ma, S.F.; Li, S.J.; Chen, F.X. Changes in the content of organic acids and expression analysis of citric acid accumulation-related genes during fruit development of yellow (*Passiflora edulis* f. *flavicarpa*) and purple (*Passiflora edulis* f. *edulis*) passion fruits. *Int. J. Mol. Sci*. **2021**, 22, 5765. https://doi.org/10.3390/ijms22115765
8. Palma, J.M.; Corpas, F.J.; Freschi, L.; Valpuesta, V. Editorial: Fruit ripening: From present knowledge to future development. *Front. Plant Sci*. **2019**, 10, 545. https://doi.org/10.3389/fpls.2022.1078841
9. Song, K.H.; Gu, H.; John, B.G.; Penta, P.; Hou, X.W.; Zhang, L.B.; Hong, K.Q.; Yao, Q.S.; Zhang, X.M. Insight into the physiological and molecular mechanisms of hot air treatment which reduce internal browning in winter-harvested pineapples. *Postharvest Biol. Technol*. **2022**, 194, 112066. https://doi.org/10.1016/j.postharvbio.2022.112066
10. Koia, J.H.; Moyle, R.L.; Botella, J.R. Microarray analysis of gene expression profiles in ripening pineapple fruit. *BMC Plant Biol*. **2012**, 12, 240. https://doi.org/10.1186/1471-2229-12-240
11. Bartolomé, A.P.; Rupérez, P.; Fúster, C. Pineapple fruit: morphological characteristics, chemical composition and sensory analysis of Red Spanish and Smooth Cayenne cultivars. *Food Chem*. **1995**, 53, 75-79. https://doi.org/10.1016/0308-8146(95)95790-D
12. Ding, P.; Syazwani, S. Physicochemical quality, antioxidant compounds and activity of MD-2 pineapple fruit at five ripening stages. *Int. Food Res. J*. **2016**, 23, 549-555. http://www.ifrj.upm.edu.my
13. Ikram, M.M.M.; Ridwani, S.; Putri, S.P.; Fukusaki, E. GC-MS based metabolite profiling to monitor ripening-specific metabolites in pineapple (*Ananas comosus*). *Metabolites*. **2020**, 10, 134. https://doi.org/10.3390/metabo10040134
14. Ikram, M.M.M.; Mizuno, R.; Putri, S.P.; Fukusaki, E. Comparative metabolomics and sensory evaluation of pineapple (*Ananas comosus*) reveal the importance of ripening stage compared to cultivar. *J. Biosci. Bioeng*. **2021**, 132, 592-598. https://doi.org/10.1016/j.jbiosc.2021.08.008
15. Hong, K.Q.; Chen, L.; Gu, H.; Zhang, X.M.; Chen, J.; Shivraj, N.; Hu, M.J.; Gong, D.Q.; Song, K.H.; Hou, X.W.; Chen, J.J.; Fan, Z.Q.; Yuan, D.B. Novel insight into the relationship between metabolic profile and fatty acid accumulation altering cellular lipid content in pineapple fruits at different stages of maturity. *J. Agric. Food Chem*. **2021**, 69, 8578-8589. https://doi.org/10.1021/acs.jafc.1c02658
16. Zhao, Y.T.; Zhu, X.; Hou, Y.Y.; Pan, Y.F.; Shi, L.; Li, X.H. Effects of harvest maturity stage on postharvest quality of winter jujube (*Zizyphus jujuba* Mill. Cv. Dongzao) fruit during cold storage. *Sci. Hortic*. **2021**, 277, 109778. https://doi.org/10.1016/j.scienta.2020.109778
17. Pillet, J.; Yu, H.W.; Chambers, A.H.; Whitaker, V.M.; Folta, K.M. Identification of candidate flavonoid pathway genes using transcriptome correlation network analysis in ripe strawberry (*Fragaria* × *nannassa*) fruit. *J. Exp. Bot*. **2015**, 66, 4455-4467. https://doi.org/10.1093/jxb/erv205
18. Zhu, X.Y.; Ye, L.L.; Ding, X.C.; Gao, Q.Y.; Xiao, S.L.; Tan, Q.Q.; Huang, J.L.; Chen, W.X.; Li, X.P. Transcriptomic analysis reveals key factors in fruit ripening and rubbery texture caused by 1-MCP in papaya. *BMC Plant Biol*. **2019**, 19, 309. https://doi.org/10.1186/s12870-019-1904-x
19. Zheng, B.B.; Zhao, L.; Jiang, X.H.; Cherono, S.; Liu, J.J.; Ogutu, C.; Ntini, C.; Zhang, X.J.; Han, Y.P. Assessment of organic acid accumulation and its related genes in peach. *Food Chem*. **2021**, 334, 127567. https://doi.org/10.1016/j.foodchem.2020.127567
20. Cai, Y.B.; Yang, X.Y.; Sun, G.M.; Zhang, Z.L.; Huang, Q.; Liu, Y.Q.; Tang, Y.Y.; Wang, Y.R.; Li, M. Relationship among colors, pigments, and antioxidant activities of pineapple leaves. *Plant Sci. J*. **2017**, 35, 283-290. http://doi.org/10.11913/PSJ.2095-0837.2017.20283
21. Liu, W.X.; Feng, Y.; Yu, S.H.; Fan, Z.Q.; Li, X.L.; Li, J.Y.; Yin, H.F. The flavonoid biosynthesis network in plants. *Int. J. Mol. Sci*. **2021**, 22, 12824. https://doi.org/10.3390/ijms22231282

22. Tohge, T.; Alseekh, S.; Fernie, A.R. On the regulation and function of secondary metabolism during fruit development and ripening. *J. Exp. Bot.* **2014**, 65, 4599-4611. https://doi.org/10.1093/jxb/ert443
23. Dong, N.Q.; Lin, H.X. Contribution of phenylpropanoid metabolism to plant development and plant-environment interactions. *J Integr. Plant Biol*. **2021**, 63, 180-209. https://doi.org/10.1111/jipb.13054
24. Saradhuldhat, P.; Paull, R.E. Pineapple organic acid metabolism and accumulation during pineapple fruit development. *Sci. Hortic.* **2007**, 112, 297-303. https://doi.org/10.1016/j.scienta.2006.12.031
25. Gao, Y.Y.; Yao, Y.L.; Chen, X.; Wu, J.Y.; Wu, Q.S.; Liu, S.H.; Guo, A.P.; Zhang, X.M. Metabolomic and transcriptomic analyses reveal the mechanism of sweet-acidic taste formation during pineapple fruit development. *Front. Plant Sci*. **2022,** 13, 971506. https://doi.org/10.3389/fpls.2022.971506
26. Geng, C.; Jin, Z.G.; Gu, M.; Li, J.B.; Tang, S.; Guo, Q.; Zhang Y.P.; Zhang, W.; Li, Y.Z.; Huang, X.N.; Lu X.F. Microbial production of *trans*-aconitic acid. *Metab. Eng*. **2023**, 78, 183-191. https://doi.org/10.1016/j.ymben.2023.06.007
27. Syazwani, S.; Nurliya, I.; Ding, P. Storage quality of 'MD-2' pineapple (*Ananas Comosus* L.) fruits. *Acta Hortic*. **2012**, 1012, 897-901. http://doi.org/10.17660/ActaHortic.2013.1012.121
28. Winkel-shirley, B. Flavonoid biosynthesis. A colorful model for genetics biochemistry, cell biology, and biotechnology. *Plant Physiol*. **2001**, 126, 485-493. https://doi.org/10.1104/pp.126.2.485
29. Albert, N.W.; Lorizzo, M.; Mengist, M.F.; Montanari, S.; Zalapa, J.; Maule, A.; Edger, P.P.; Yocca, A.E.; Platts, A.E.; Pucker, B.; Espley, R.V. Vaccinium as a comparative system for understanding of complex flavonoid accumulation profiles and regulation in fruit. *Plant Physiol*. **2023**, 192, 1696-1710. https://doi.org/10.1093/plphys/kiad250
30. Wang, L.X.; Chen, M.X.; Lam, P.Y.; Dini-Andreote, F.; Dai, W.; Wei, Z. Multifaceted roles of flavonoids mediating plant-microbe interactions. *Microbiome*. **2022**, 10, 233. https://doi.org/10.1186/s40168-022-01420-x
31. Yuan, L.; Niu, H.H.; Yun, Y.R.; Tian, J.; Lao, F.; Liao, X.J.; Gao, Z.Q.; Ren, D.B.; Zhou, L.Y. Analysis of coloration characteristics of Tunisian soft-seed pomegranate arils based on transcriptome and metabolome. *Food Chem*. **2022**, 370, 131270. https://doi.org/10.1016/j.foodchem.2021.131270
32. Qian, M.J.; Wu, H.X.; Yang, C.K.; Zhu, W.C.; Shi, B.; Zheng, B.; Wang, S.B.; Zhou, K.B.; Gao, A.P. RNA-seq reveals the key pathways and genes involved in the light-regulated flavonoids biosynthesis in mango (*Mangifera indica* L.) peel. *Front. Plant Sci.* **2023**, 13, 1119384. https://doi.org/10.3389/fpls.2022.1119384
33. Xu, B.; Escamilla-Treviño, L.L.; Sathitsuksanoh, N.; Shen, Z.X.; Shen, H.; Zhang, Y.P.; Dixon, R.A.; Zhao, B.Y. Silencing of 4-coumarate:coenzyme A ligase in switchgrass leads to reduced lignin content and improved fermentable sugar yields for biofuel production. *New Phytol*. **2011**, 192, 611-625. https://doi.org/10.1111/j.1469-8137.2011.03830.x
34. Eudes, A.; Pereira, J.H.; Yogiswara, S.; Wang, G.; Benites, V.T.; Baidoo, E.E.K.; Lee, T.S.; Adams, P.D.; Keasling, J.D.; Loqué, D. Exploiting the substrate promiscuity of hydroxycinnamoyl-CoA: shikimate hydroxycinnamoyl transferase to reduce lignin. *Plant Cell Physiol*. **2016**, 57, 568-579. https://doi.org/10.1093/pcp/pcw016
35. Yang, T.T.; Zhang, P.Y.; Pan, J.H.; Amanullah, S.; Luan, F.S.; Han, W.H.; Liu, H.Y.; Wang, X.Z. Genome-wide analysis of the peroxidase gene family and verification of lignin synthesis-related genes in watermelon. Int. J. Mol. Sci. 2022, 23(2), 642. https://doi.org/10.3390/ijms23020642
36. Kumari, A.; Dogra, V.; Joshi, R.; Kumar, S. Stress-responsive *cis*-regulatory elements underline podophyllotoxin biosynthesis and better performance of *Sinopodophyllum hexandrum* under water deficit conditions. *Front. Plant Sci*. **2022**, 12, 2021. https://doi.org/10.3389/fpls.2021.751846
37. Tanaka, N.; Murao, S. Difference between various copper-containing enzymes (*Polyporus* Laccase, Mushroom Tyrosinase and Cucumber Ascorbate Oxidase) and Bilirubin Oxidase. *Agric. Biol. Chem*. **1983**, 47, 1627-1628. https://doi.org/10.1080/00021369.1983.10865827
38. Sadka, A.; Dahan, E.; Cohen, E.L.; March, K. Aconitase activity and expression during the development of lemon fruit. *Physiol Plant.* **2000**, 108, 255-262. https://doi.org/10.1034/j.1399-3054.2000.108003255.x
39. Hong, K.Q.; Yao, Q.S.; Golding, J.B.; Pristijono, P.; Zhang, X.M.; Hou, X.W.; Yuan, D.B.; Li, Y.X.; Chen, L.; Song, K.H.; Chen, J. Low temperature storage alleviates internal browning of 'Comte de Paris' winter pineapple fruit by reducing phospholipid degradation, phosphatidic acid accumulation and membrane lipid peroxidation processes. *Food Chem*. **2023**, 404, 134656. https://doi.org/10.1016/j.foodchem.2022.134656
40. Li, B.Y.; Li, H.; Xu, Z.H.; Guo, X.N.; Zhou, T.; Shi, J.L. Transcriptome profiling and identification of the candidate genes involved in early ripening in *Ziziphus Jujuba*. *Front. Genet*. **2022**, 13, 863746. https://doi.org/10.3389/fgene.2022.863746
41. Hou, X.W.; Lu, Z.W.; Hong, K.Q.; Song, K.H.; Gu, H.; Hu, W.; Yao, Q.S. The class III peroxidase gene family is involved in ascorbic acid induced delay of internal browning in pineapple. *Front. Plant Sci*. **2022**, 13, 953623. https://doi.org/10.3389/fpls.2022.953623
42. Zhou, F.H.; Xu, D.Y.; Liu, C.H.; Chen, C.; Tian, M.X.; Jiang, A.L. Ascorbic acid treatment inhibits wound healing of fresh-cut potato strips by controlling phenylpropanoid metabolism. *Postharvest Biol. Technol*. **2021**, 181, 111644. https://doi.org/10.1016/j.postharvbio.2021.111644

43. Morrison, I.M. A semi-micro method for the determination of lignin and its use in predicting the digestibility of forage Crops. *J. Sci. Food Agric*. **1972**, 23, 455-463. https://doi.org/10.1002/jsfa.2740230405
44. Langfelder, P.; Horvath, S. WGCNA: An R package for weighted correlation network analysis. *BMC Bioinformatics*. **2008**, 9, 559. https://doi.org/10.1186/1471-2105-9-559
45. Livak, K.J.; Schmittgen, T.D. Analysis of relative gene expression data using real-time quantitative PCR and the $2^{-\triangle\triangle CT}$ method. *Methods*, **2001**, 25, 402-408. https://doi.org/10.1006/meth.2001.1262